molecular oral microbiology

molecular oral microbiology

Analysis of *Porphyromonas gingivalis* PG27 by deletion and intragenic suppressor mutation analyses

I. Ishiguro, K. Saiki and K. Konishi

Department of Microbiology, Nippon Dental University School of Life Dentistry at Tokyo, Tokyo, Japan

Correspondence: Keitarou Saiki, Department of Microbiology, Nippon Dental University School of Life Dentistry at Tokyo, 1-9-20 Fujimi, Chiyoda-ku, Tokyo 102-8159, Japan Tel.: +81 3 3261 8763; fax: +81 3 3264 8399; E-mail: keisaiki@tky.ndu.ac.jp

Keywords: gingipain; lipopolysaccharide; *Porphyromonas*; secretion

Accepted 17 June 2011
DOI: 10.1111/j.2041-1014.2011.00620.x

SUMMARY

PG27 is required for secretion of virulence factor gingipains, and has recently been proposed as LptO, which is involved in *O*-deacylation of lipopolysaccharide. In the present study, a predicted 14 anti-parallel β-strand structure of PG27 was ascertained. Deletion study showed that the region from Asp382 to the C-terminal His391 of PG27 is dispensable for the function of PG27. Analysis of C-terminal deletion mutants revealed that the region in strand S14 (Asn369–Gly385) is important for activity. Of the gingipain-defective mutants, ΔThr378–His391 and ΔPhe377–His391 produced amounts of PG27 comparable to those produced by wild-type cells, suggesting that Thr378–Phe381 contains essential residues for the function of PG27. In contrast, ΔPhe381–His391, ΔAla380–His391, ΔLeu379–His391 and ΔArg376–His391 produced no detectable PG27. The defects of the ΔAla380–His391 mutant were suppressed by changing either Ala346 or Ala359 of PG27 to valine. Importantly, Ala346 and Ala359 are located close to Leu379 in the structural model of PG27. A359V compensated for the instability of PG27, but not the gingipain-defective phenotypes, of other deletion mutants tested, suggesting that Ala380 and Phe381 of PG27 are important for the stability of PG27. Lastly, we found that the C-terminal region of PG27 may be located in the periplasm. Taken together, these findings fit well with a predicted β-barrel structure model for PG27, and show that strand S14 is important for its function.

INTRODUCTION

The gram-negative anaerobe *Porphyromonas gingivalis* is increased in subgingival biofilms, often associated with *Tannerella forsythia* and *Treponema denticola* (red-complex periopathogens), and occasionally causes aggressive and chronic periodontitis (Christersson *et al.*, 1992; Socransky & Haffajee, 1992; Darveau, 2010). Chronic inflammation accompanied by the destruction of human periodontal tissue is the typical pathology of aggressive and chronic periodontitis, and would be inevitably brought about by accelerated growth of this bacterium in the periodontium. *Porphyromonas gingivalis* is asaccharolytic and uses short-chain peptides as its sole energy source (Takahashi & Sato, 2001). In an oral environment where short-chain peptides are not abundant, proliferation of *P. gingivalis* is deemed to rely on nascent hydrolysates of external proteins. Accordingly, *P. gingivalis* secretes various types of endopeptidases [Arg-gingipains (RgpA and RgpB) and Lys-gingi-

pain (Kgp)] and exopeptidases (DPP IV, DPP-7, PTP-A, CPG70; Banbula *et al.*, 1999, 2000, 2001; Curtis *et al.*, 1999; Chen *et al.*, 2002). The roles of these secreted proteases in the growth of *P. gingivalis* have been thoroughly investigated. Oda *et al.* (2007, 2009) developed a minimal medium that contains bovine γ-immunoglobulin and bovine serum albumin as the sole energy source (GA medium); they examined the growth properties of *P. gingivalis* protease-defective mutants, and concluded that Arg-gingipains and Lys-gingipains are essential for growth in this medium. The evidence indicates that gingipains are important factors for the proliferation of this bacterium. Furthermore, excessive proliferation of this bacterium in the periodontium may cause synergistic destruction of the periodontal tissue. Therefore, gingipains are also virulence factors of this bacterium.

Elucidation of the mechanism of the secretion of gingipains is an important issue to be addressed. Many proteins have been reported to be involved in the production of active gingipains. PorX, PorY and GppX are putative two-component system regulatory proteins (Hasegawa *et al.*, 2003; Sato *et al.*, 2010). VimA, VimE, VimF, PorR, Rfa and GtfB are the enzymes for carbohydrate modification of gingipains and the biosynthesis of lipopolysaccharide (LPS; Abaibou *et al.*, 2001; Shoji *et al.*, 2002; Vanterpool *et al.*, 2004, 2005a,b; Sato *et al.*, 2009). PorK, PorL, PorM, PorN, PorP, PorT, PorW and Sov are proposed as the proteins of the Por secretion system (PorSS; Sato *et al.*, 2005, 2010; Saiki & Konishi, 2007). Gingipains may cross the inner membrane via the Sec system followed by transport across the outer membrane via a putative protein secretion system, PorSS, which was originally proposed as an orthologous secretion system for the gliding motility of *Flavobacterium johnsoniae* (Sato *et al.*, 2010). PorK-N, PorP, PorT, PorW and Sov exhibit no sequence similarity to any component of the conserved bacterial protein secretion systems, supporting the proposal that PorSS is a novel protein secretion system (Sato *et al.*, 2005, 2010; Saiki & Konishi, 2007). PG27, PorU, PorQ and PG534 are additional proteins that may participate in some steps for generation of active gingipains (Ishiguro *et al.*, 2009; Saiki & Konishi, 2010b; Sato *et al.*, 2010).

In a previous study, we identified PG27 as a novel membrane protein of *P. gingivalis* W83 (Ishiguro *et al.*, 2009). A PG27-defective mutant showed a phenotype similar to that of a Sov-defective mutant (Saiki & Konishi, 2010b), suggesting that PG27 is involved in the secretion of gingipains. It has been proposed that LPS deacylation is linked to the secretion of the C-terminal domain proteins such as gingipains, and that PG27/LptO is involved in the *O*-deacylation of LPS (Chen *et al.*, 2011). A comparative model for PG27/LptO has also been generated from the structure of the fatty acid transporter FadL from *Escherichia coli* (van den Berg *et al.*, 2004), leading to the proposal that PG27/LptO forms a 14-stranded β-barrel (Chen *et al.*, 2011). In the present study, we investigated the effects of deletion and suppressor mutations in the C-terminal region of PG27.

METHODS

Bacterial strains, plasmids and growth media

Strains and plasmids are listed in Table 1. *Escherichia coli* ER2566 (New England Biolabs, Ipswich, MA) was grown in Luria–Bertani broth. *Porphyromonas gingivalis* was routinely cultured anaerobically (10% CO_2, 10% H_2 and 80% N_2) at 37°C in brain–heart infusion (Becton Dickinson, Franklin Lakes, NJ) supplemented with haemin (7.67 μM) and menadione (2.91 μM; BHIHM). Before *P. gingivalis* cell cultures were used in experiments, the turbidity was adjusted to an optical density at 600 nm (OD_{600}) of 1.0 using a SmartSpec Plus spectrophotometer (Bio-Rad, Hercules, CA). In examining the ability for black-pigmentation of *P. gingivalis*, BHIHM agar supplemented with defibrinated horse blood [5% volume/volume (v/v)] (blood agar) was used. To isolate suppressor mutants of *P. gingivalis* mutants, a minimal medium GA agar [10 mM NaH_2PO_4, 10 mM KCl, 10 mM $MgCl_2$, 22.5 mg ml^{-1} bovine γ-immunoglobulin (Sigma-Aldrich, St Louis, MO), 7.5 mg ml^{-1} bovine serum albumin (Sigma-Aldrich), 7.67 μM haemin and 2.91 μM menadione, 1.5% weight/volume (w/v) agar, pH 7.0; (Oda *et al.*, 2007)] was used. Ampicillin (100 μg ml^{-1}) and erythromycin (5 μg ml^{-1}) were added to the medium as needed.

Construction of PG27 deletion mutants

Polymerase chan reaction (PCR) was performed with Vent DNA polymerase (New England Biolabs). A 0.3-kilobase pair (kbp) 3′-terminal region of the *PG0027*

Table 1 *Porphyromonas gingivalis* strains and pUC119 plasmid derivatives used in this study

Strain or plasmid	Genotype or description	Source
Strains		
W83	*-PG26-PG27-PG28-* (wild-type)	Laboratory stock
83K10	*-PG26-erm-PG28-*	Ishiguro *et al.* (2009)
83K12	*-PG26-PG27-erm-PG28-*	Ishiguro *et al.* (2009)
83K13	*-PG26-PG27[Δ309-391]-erm-PG28-*	Ishiguro *et al.* (2009)
83K27	*-PG26-PG27[Δ325-391]-erm-PG28-*	Present study
83K28	*-PG26-PG27[Δ342-391]-erm-PG28-*	Present study
83K29	*-PG26-PG27[Δ359-391]-erm-PG28-*	Present study
83K30	*-PG26-PG27[Δ376-391]-erm-PG28-*	Present study
83K31	*-PG26-PG27[Δ377-391]-erm-PG28-*	Present study
83K32	*-PG26-PG27[Δ378-391]-erm-PG28-*	Present study
83K33	*-PG26-PG27[Δ379-391]-erm-PG28-*	Present study
83K34	*-PG26-PG27[Δ380-391]-erm-PG28-*	Present study
83K35	*-PG26-PG27[Δ381-391]-erm-PG28-*	Present study
83K36	*-PG26-PG27[Δ382-391]-erm-PG28-*	Present study
83K37	*-PG26-PG27[Δ387-391]-erm-PG28-*	Present study
83K38	*-PG26-PG27[Δ380-391, A346V]-erm-PG28-*	Present study
83K39	*-PG26-PG27[Δ380-391, A359V]-erm-PG28-*	Present study
83K40	*-PG26-PG27[Δ380-391 + RYPR]-erm-PG28-*[1]	Present study
83K41	*-PG26-PG27[Δ381-391 + Y]-erm-PG28*[2]	Present study
83K42	*-PG26-PG27[A359V]-erm-PG28-*	Present study
83K43	*-PG26-PG27[Δ376-391, A359V]-erm-PG28-*	Present study
83K44	*-PG26-PG27[Δ377-391, A359V]-erm-PG28-*	Present study
83K45	*-PG26-PG27[Δ378-391, A359V]-erm-PG28-*	Present study
83K46	*-PG26-PG27[Δ379-391, A359V]-erm-PG28-*	Present study
83K47	*-PG26-PG27[Δ381-391, A359V]-erm-PG28-*	Present study
83K48	*-PG26-PG27HisTag-erm-PG28-*[3]	Present study
Plasmids		
pUC119	Ap^r	Sambrook *et al.* (1989)
pKS1	*lacZ*::*erm*	Saiki & Konishi (2007)
pKS11	*lacZ*::*erm*	Saiki & Konishi (2007)
pKS16	*PG27-erm-PG28*	Ishiguro *et al.* (2009)
pKS47	*PG27[Δ325-391]-erm-PG28*	Present study
pKS48	*PG27[Δ342-391]-erm-PG28*	Present study
pKS49	*PG27[Δ359-391]-erm-PG28*	Present study
pKS50	*PG27[Δ376-391]-erm-PG28*	Present study
pKS51	*PG27[Δ377-391]-erm-PG28*	Present study
pKS52	*PG27[Δ378-391]-erm-PG28*	Present study
pKS53	*PG27[Δ379-391]-erm-PG28*	Present study
pKS54	*PG27[Δ380-391]-erm-PG28*	Present study
pKS55	*PG27[Δ381-391]-erm-PG28*	Present study
pKS56	*PG27[Δ382-391]-erm-PG28*	Present study
pKS57	*PG27[Δ387-391]-erm-PG28*	Present study
pKS58	*PG27[Δ380-391, A346V]-erm-PG28*	Present study
pKS59	*PG27[Δ380-391, A359V]-erm-PG28*	Present study
pKS60	*PG27[Δ380-391 + RYPR]-erm-PG28*[1]	Present study
pKS61	*PG27[Δ381-391 + Y]-erm-PG28*[2]	Present study
pKS62	*PG27[A359V]-erm-PG28*	Present study
pKS63	*PG27[Δ376-391, A359V]-erm-PG28*	Present study
pKS64	*PG27[Δ377-391, A359V]-erm-PG28*	Present study
pKS65	*PG27[Δ378-391, A359V]-erm-PG28*	Present study
pKS66	*PG27[Δ379-391, A359V]-erm-PG28*	Present study
pKS67	*PG27[Δ381-391, A359V]-erm-PG28*	Present study
pKS68	*PG27HisTag-erm-PG28*[3]	Present study

erm, *ermF-ermAM*; Ap^r, ampicillin-resistant; numbers in brackets indicate amino acid residues.
[1]The C-terminal sequence of PG27 is Leu379-Arg380-Tyr381-Pro382-Arg383.
[2]The C-terminal sequence of PG27 is Leu379-Ala380-Tyr381.
[3]*HisTag*, a histidine-tag [-Thr-Ser-$(His)_{12}$] fused to the 3′ terminus of PG27.

gene was amplified by PCR with 5′-GGGTAATGCGGAGAGCTTGTGGTCGTTGGG-3′ and 5′-TT*GGTACC*TATTTATCGTCATAGCTATATT-3′ (italics indicate *Kpn*I site). The PCR product was digested with *Bgl*II (in the *PG0027*) and *Kpn*I, and cloned into the 3.6-kbp *Bgl*II-*Kpn*I-digested *ermF-ermAM-PG0028* fragment from pKS16 (Ishiguro *et al.*, 2009) to create pKS47, in which 0.25 kbp of the 3′ terminus of *PG0027* is deleted. pKS48-pKS57 were similarly constructed by ligation of the 3.6-kbp *Bgl*II-*Kpn*I-digested *ermF-ermAM-PG0028* fragment from pKS16 and the *Bgl*II-*Kpn*I-digested PCR products, which were amplified with 5′-GGGTAATGCGGAGAGCTTGTGGTCGTTGGG-3′ and the following primers: 5′-TT*GGTACC*TACAAATTGCCTTTGGTGGGGT-3′ (italics: *Kpn*I site; for pKS48), 5′-TT*GGTACC*TAATCGATACGGAATATGTTCA-3′ (italics: *Kpn*I site; for pKS49), 5′-TT*GGTACC*TACAGAGTCTGATCCAACGGAT-3′ (italics: *Kpn*I site; for pKS50), 5′-AT*GGTACC*TACCGCAGAGTCTGATCCAACG-3′ (italics: *Kpn*I site; for pKS51), 5′-AT*GGTACC*TAAAACCGCAGAGTCTGATCCA-3′ (italics: *Kpn*I site; for pKS52), 5′-TT*GGTACC*TACGTAAACCGCAGAGTCTGAT-3′ (italics: *Kpn*I site; for pKS53), 5′-TT*GGTACC*TAAAGCGTAAACCGCAGAGTCT-3′ (italics: *Kpn*I site; for pKS54), 5′-AT*GGTACC*TAAGCAAGCGTAAACCGCAGAG-3′ (italics: *Kpn*I site; for pKS55), 5′-TT*GGTACC*TAGAAAGCAAGCGTAAACCGCA-3′ (italics: *Kpn*I site; for pKS56) and 5′-TT*GGTACC*TACAATCCATCCATATCGAAAG-3′ (italics: *Kpn*I site; for pKS57). pKS47, pKS48, pKS49, pKS50, pKS51, pKS52, pKS53, pKS54, pKS55, pKS56 and pKS57 were linearized and used to construct *P. gingivalis* mutants 83K27, 83K28, 83K29, 83K30, 83K31, 83K32, 83K33, 83K34, 83K35, 83K36 and 83K37, respectively, by electroporation (Saiki & Konishi, 2007). Deletion mutations of 83K27–83K37 were confirmed by determining the nucleotide sequences of the DNA regions that were PCR amplified.

Isolation of spontaneous suppressor mutants and construction of suppressor/deletion double mutants of PG27

The *Porphyromonas gingivalis* mutant cell cultures (2 ml) were centrifuged. The cell pellets (4×10^9 to 6×10^9 cells) were washed, suspended in phosphate-buffered saline (PBS), plated onto GA agar, and incubated anaerobically at 37°C for up to 2 months. Spontaneous suppressor mutants of a *P. gingivalis* deletion mutant were isolated as colony-forming cells on GA agar. The nucleotide sequences for the *PG0027* gene of suppressor mutants were confirmed as described above. A 3′-terminal region of the *PG0027* gene carrying both a spontaneous mutation and the original deletion mutation was amplified by PCR with 5′-GGGTAATGCGGAGAGCTTGTGGTCGTTGGG-3′ and 5′-GCTCTAGATCTACGAAGGATGAAATTTTTCAGG-3′. The PCR product was digested with *Bgl*II (in the *PG0027*) and *Kpn*I (between the *PG0027* and *ermF*), and cloned into the 3.6-kbp *Bgl*II-*Kpn*I-digested *ermF-ermAM-PG0028* fragment from pKS16 to create pKS58–pKS61. pKS58, pKS59, pKS60 and pKS61 (Table 1) were linearized and used to construct *P. gingivalis* mutants 83K38, 83K39, 83K40 and 83K41, respectively, by electroporation. These *P. gingivalis* mutants were designated as suppressor/deletion double mutants.

Construction of PG27 double mutants and other PG27 mutants

To introduce the suppressor mutation A359V into other *PG0027* deletion mutants, pKS59 was digested with *Alw*NI (one in the vector and one in *PG0027*), and a 2.8-kbp fragment including *PG0027* with the suppressor mutation for A359V was isolated. The 2.8-kbp *Alw*NI-digested fragment was ligated with the 3.4-kbp *Alw*NI-digested *erm-PG0028*-vector fragment from pKS16, pKS50, pKS51, pKS52, pKS53 and pKS55, constructing pKS62, pKS63, pKS64, pKS65, pKS66 and pKS67, respectively. pKS62, pKS63, pKS64, pKS65, pKS66 and pKS67 were linearized and used to construct *P. gingivalis* mutants 83K42, 83K43, 83K44, 83K45, 83K46 and 83K47, respectively, by electroporation. These *P. gingivalis* mutants were designated as A359V/deletion double mutants. To introduce a histidine-tag to the 3′ terminus of PG27, an annealed-oligonucleotide linker (5′-CTAGTCATCACCATCACCATCACCATCACCATCACCATCACTAG-3′/5′-TCGACTAGTGATGGTGATGGTGATGGTGATGGTGATGGTGATGA-3′) was ligated with the 4.2-kbp *Spe*I-*Sal*I-digested *PG0027-PG0028* fragment from pKS16 (Ishiguro *et al.*, 2009). The resultant plasmid was digested with *Pst*I and ligated with the 2.2-kbp *Pst*I-digested *ermF-ermAM* fragment from pKS11 (Ishiguro *et al.*, 2009) to create pKS68,

in which *ermF-ermAM* was inserted in the forward orientation. pKS68 was linearized and used to construct *P. gingivalis* mutants 83K48 by electroporation. The introduced mutations of 83K42–48 were confirmed similarly as described above.

Preparation of subcellular fractions and enzymatic assays

The *Porphyromonas gingivalis* culture was centrifuged at 10,000 ***g*** for 5 min at 4°C, and the supernatant was collected (the extracellular fraction). The harvested cells were washed with PBS (137 mM NaCl, 2.7 mM KCl, 4.3 mM Na_2HPO_4 and 1.4 mM KH_2PO_4), suspended in PBS, and sonicated (Ultrasonic generator US-150 with tip #7; Nihonseiki, Japan) to generate the cell extract fraction. Rgp activity was determined in Tris–HCl (100 mM, pH 8.0) -$CaCl_2$ (10 mM) -L-cysteine (10 mM) using 0.4 mM *N*-α-benzoyl-DL-Arg 4-nitroanilide (Sigma-Aldrich). Kgp activity was determined in sodium phosphate (20 mM, pH 7.5) -L-cysteine (5 mM) using 0.2 mM *N*-*p*-tosyl-Gly-Pro-Lys 4-nitroanilide (Sigma-Aldrich). The reactions were performed at 37°C, and absorbance at 405 nm was measured with a SPECTRA max 384 plus (Molecular Devices, Sunnyvale, CA). Statistically significant differences in the median values were evaluated using the Mann–Whitney *U*-test. Differences were considered statistically significant at $P < 0.01$.

Preparation of subcellular fractions and immunoblot analyses

The *Porphyromonas gingivalis* cultures were centrifuged at 10,000 ***g*** for 5 min at 4°C, and supernatants were collected. A 6-ml portion of the extracellular fraction was concentrated to 0.1 ml on ultrafiltration membranes (10,000 molecular weight cut-off; Sartorius Stedim Biotech, Aubagne, France), diluted with 8 M urea (3 ml) supplemented with protease inhibitor cocktail (PIC; 1%, v/v), which is a mixture of protease inhibitors [4-(2-aminoethyl)-benzensulphonyl fluoride (104 mM), aprotinin (0.08 mM), leupeptin (2.1 mM), bestatin (3.6 mM), pepstatin A (1.5 mM), E-64 (1.4 mM), and *N*-α-*p*-tosyl-L-lysine chloromethyl ketone hydrochloride (0.1 mM; Sigma-Aldrich)], and concentrated to 0.1 ml. The harvested cells were washed with PBS supplemented with PIC (1%, v/v; PBS/PIC), suspended in PBS/PIC, sonicated, and were ultracentrifuged at 104,000 ***g*** for 30 min at 4°C. The supernatant was removed, and the pellets were suspended in PBS/PIC containing 0.1% sodium dodecyl sulphate (SDS; the total membrane fraction).

Quantification of transcripts by RT-PCR

Cell lysates were prepared from *P. gingivalis* cells using RNAprotect Bacterial Reagent (Qiagen GmbH, Hilden, Germany), and total RNA was isolated using an RNeasy Mini kit with RNase-Free DNase Set (both Qiagen). RNA was quantified spectrophotometrically as 44 μg ml^{-1}·absorbance at 260 nm. Reverse transcription and PCR amplification were performed using a OneStep RT-PCR kit (Qiagen), according to the manufacturer's protocol using 5′-GGGTAATGCGGAGAGCTTGTGGTCGTTGGG-3′ and 5′-TTGGTACCTACGTAAACCGCAGAGTCTGAT-3′ for amplification of a 0.3-kbp 3′-terminal region of the *PG0027* gene, and 5′-CTTGAGTTCAGTGGCGGCAG-3′ and 5′-AGGGAAGACGGTTTTCACCA-3′ for amplification of the 0.4-kbp central region of the 16S ribosomal RNA gene. The PCR products were separated by agarose gel electrophoresis and visualized by staining with ethidium bromide.

Orientation of the C-terminal portion of PG27

Cells from 2-ml cultures of 83K48 were treated with porcine pancreatic trypsin (2.5 mg ml^{-1}; Wako Pure Chemical, Osaka, Japan) or proteinase K from *Tritirachium album* (0.5 mg ml^{-1}; Sigma-Aldrich) in PBS (0.2 ml) supplemented with or without Triton X-100 (0.1%, w/v) for 30 min at 37°C. After incubation, the cell mixture was mixed with urea (0.2 g) and PIC (10 μl), treated with Triton X-100 (2%, w/v), sonicated and centrifuged (10,000 ***g*** for 5 min at 4°C) to remove cell debris. Histidine-tagged PG27 or its C-terminal hydrolysates were purified using Ni^{2+}-chelated Sepharose Fast Flow (GE Healthcare UK Ltd., Buckinghamshire, UK) under denaturing conditions, according to the manufacturer's protocol, and detected by Western blot analysis using anti-PG27 antiserum.

Homology modelling of PG27

A comparative model for PG27 from the known 1t16 structure (fatty acid transporter FadL from *E. coli*; van den Berg *et al.*, 2004; Chen *et al.*, 2011) was

constructed using the computer program MODELLER version 9v8 (Šali & Blundell, 1993), and assessed using the DOPE (discrete optimized protein energy) method (Shen & Sali, 2006) and the GA341 method (Melo *et al.*, 2002; John & Sali, 2003). The three-dimensional structures of PG27 were drawn using MOLFEAT v4.5 (FiatLux Co., Tokyo, Japan).

Western blot analysis

Protein samples were mixed in Tris–HCl (65 mM, pH 6.8) -SDS (3%, w/v) -glycerol (10%, w/v) -PIC (1%, v/v), incubated for 10 min at 90°C, mixed with dithiothreitol (100 mM), and immediately subjected to 10% SDS–polyacrylamide gel electrophoresis. Separated proteins were transferred to a 0.45-μm nitrocellulose membrane (Whatman plc, Kent, UK). Arg-gingipains, Lys-gingipain and PG27 were detected using anti-RgpB antiserum (Ishiguro *et al.*, 2009), anti-Kgp antiserum (Saiki & Konishi, 2010a) and anti-PG27 antiserum (Ishiguro *et al.*, 2009), respectively, as primary antibodies, and visualized using horseradish peroxidase-conjugated goat anti-rabbit IgG (Bio-Rad) as a secondary antibody.

RESULTS

Construction of PG27 C-terminal deletion mutants

A structural model for the PG27 protein of *P. gingivalis* W83 shows 14 anti-parallel strands S1–S14 (Fig. 1A). To verify this β-barrel structural model, we conducted a deletion study in the C-terminal region of PG27 to define the regions of PG27 essential for its function (Fig. 1B). 83K13 has strands S10–S14 deleted (Ishiguro *et al.*, 2009). 83K27, 83K28 and 83K29 have strands S11–S14, S12–S14 and S13–S14 deleted, respectively. 83K30–83K36 have strand S14 partially deleted. 83K37 has the C-terminal portion of PG27 deleted. The effects of the deletion mutations on gingipain activity were assessed in an assay in which the formation of black-pigmented colonies on blood agar is dependent on the activity of the gingipains (Shi *et al.*, 1999). As shown in Fig. 1(C), wild-type W83 and an insertion control, 83K12, in which the *ermF-ermAM* cassette was inserted between *PG0027* and *PG0028*, formed black-pigmented colonies, whereas 83K10 (Δ*PG0027*) forms white colonies (Ishiguro *et al.*, 2009). 83K36 and 83K37 (Fig. 1B) formed black-pigmented colonies (Fig. 1C), whereas 83K27–83K33 and 83K35 (Fig. 1B) formed white colonies (Fig. 1C). The mutant 83K34 (Fig. 1B) produced pale grey colonies (Fig. 1C). These results show that the C-terminal portion corresponding to strand S14 of PG27 is important for black-pigmentation of *P. gingivalis.*

Characterization of PG27 C-terminal deletion mutants

Because black pigmentation of *P. gingivalis* colonies can be affected by several mechanisms, we assessed the gingipain activity in cell extract fractions and extracellular fractions from PG27 deletion mutants (Fig. 2A). The activities of Arg-gingipains and Lys-gingipain were similar in both fractions from W83 and 83K12 (83–104%), indicating that the insertion of the *ermF-ermAM* cassette between *PG0027* and *PG0028* has little effect on the biogenesis of gingipains. Deletion of up to 10 amino acids resulted in modest reduction in Lys-gingipain in cell extract (44% of that of 83K12, $P < 0.01$). In contrast, deletion of 11 or more amino acids resulted in nearly complete loss of gingipain activity in both the extracellular fraction and in the cell extract fraction. A small amount of activity remained (4–8% of those of 83K12, $P < 0.01$) for 83K34, which had 12 amino acids deleted. This is consistent with the residual gingipain activity as measured by the colony assay (Fig. 1C).

Extracellular fractions from PG27 deletion mutants were prepared and subjected to Western blot analysis using anti-RgpB antiserum (Fig. 2B) or anti-Kgp antiserum (Fig. 2C). Arg-gingipains were detected as a 42-kDa catalytic domain form and as 70–90-kDa glycosylated forms (Potempa *et al.*, 1995; Nakayama, 1997; Seers *et al.*, 2006) in W83 and 83K12 (Fig. 2B, lanes 1 and 2). Similar protein bands were also detected in 83K36 and 83K37 (Fig. 2B, lanes 5 and 4), suggesting that Arg-gingipains were properly secreted in these mutants. In contrast, Arg-gingipains were barely detected as protein bands near 58, 54 and/or 45 kDa in 83K10 (Fig. 2B, lane 3; too faint to detect), 83K13, 83K30–33 and 83K35 (lanes 12, 11–8, and 6), or as a faint 46-kDa protein band in 83K34 (lane 7). These mutants exhibited poor Arg-gingipain activity in the extracellular fractions (0–3% of that of 83K12 in Fig. 2A), 58-, 54-, and 45-kDa Arg-gingipains were afunctional and probably degradation

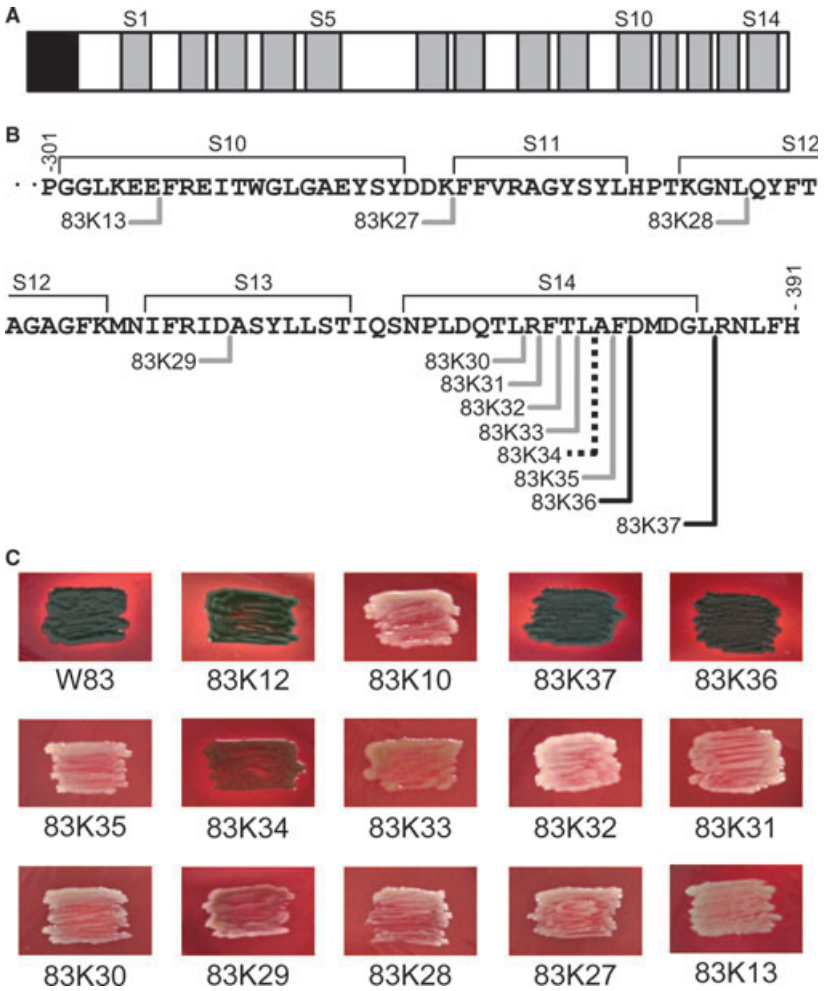

Figure 1 (A) Diagram of the secondary structure of PG27. Grey rectangles indicate predicted strands of the 14 anti-parallel β-barrel structural model. The black rectangle indicates a putative signal sequence. (B) The C-terminal region of PG27 [first line, Pro301-Thr345; second line, Ala346–His391 (the C-terminus)]. The C-termini of the deletion mutants are indicated by grey hooked-lines (afunctional), a dotted line (barely active), or a black line (active). Strands S10–S14 are indicated above the lines. (C) Accumulation of black pigmentation of PG27 C-terminal deletion mutants (83K13, 83K27–83K37), Δ*PG0027* mutant (83K10), insertion control (83K12), and wild-type (W83), grown on blood agar.

products of Arg-gingipains. These results indicate that Arg-gingipains are barely secreted in PG27-defective mutants. The expression of Lys-gingipains in the extracellular fractions is shown in Fig. 2(C). Lys-gingipains were detected as a 47-kDa catalytic domain form (Vanterpool *et al.*, 2005a) in W83 and 83K12 (Fig. 2C, lanes 1 and 2). 83K36 and 83K37 also produced 47-kDa Lys-gingipains in the extracellular fractions (Fig. 2C, lanes 5 and 4). In contrast, the Lys-gingipain protein band was not detected in 83K10, 83K13, 83K30–33 and 83K35 (Fig. 2C, lanes 3, 12, 11–8, and 6). In 83K34, the 47-kDa Lys-gingipain protein band was barely detected (Fig. 2C, lane 7), suggesting that 83K34 secretes a small amount of Lys-gingipain. This result is consistent with the very low activity of Lys-gingipain in the extracellular fraction of 83K34 (4% of that of 83K12 shown in Fig. 2 A). These results show that Lys-gingipains are barely secreted in PG27-defective mutants.

Total membrane fractions from PG27 deletion mutants were prepared and subjected to Western blot analysis using anti-PG27 antiserum (Fig. 2D). W83 and 83K12 produced 39-kDa PG27 proteins (Fig. 2D, lanes 1 and 2), whereas 83K10 did not (lane 3; Ishiguro *et al.*, 2009). Bands apparently corresponding to truncated proteins were detected in

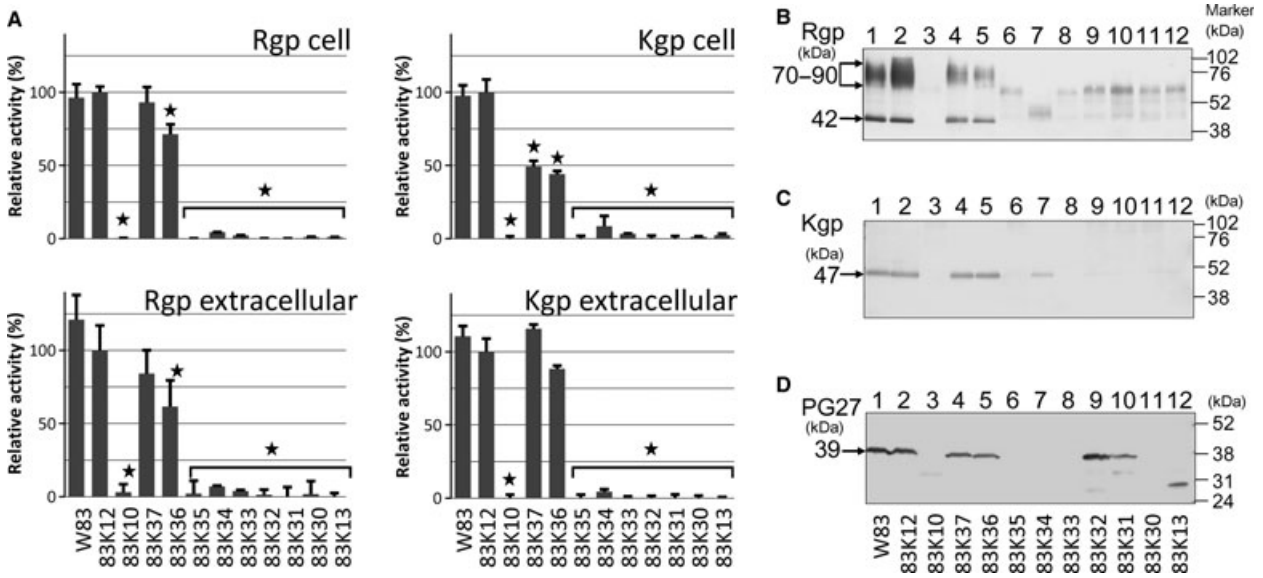

Figure 2 Gingipain expression (A–C) and PG27 expression (D) in PG27 C-terminal deletion mutants. (A) Activities of Arg-gingipains (Rgp) and Lys-gingipain (Kgp) in cell extract fractions (cell) or extracellular fractions (extracellular). Six measurements were collected from two experiments. *Significant difference compared with 83K12, $P < 0.01$. Error bars indicate SD (calculated from the enzyme activity). Protease activity is indicated relative to 83K12 (set at 100%); the absolute values of Rgp/cells, Rgp/extracellular, Kgp/cells and Kgp/extracelluar are 83.8, 31.8, 9.86 and 3.13 ΔA_{405} h^{-1} ml^{-1} $OD_{600}{}^{-1}$, respectively. (B–D) Extracellular fractions (B, C) or total membrane fractions (D) were subjected to 10% sodium dodecyl sulphate–polyacrylamide gel electrophoresis, followed by immunoblot analysis with anti-Rgp antiserum (B), anti-Kgp antiserum (C), or anti-PG27 antiserum (D). Molecular mass markers are on the right. Arrows on the left are the positions of mature Arg-gingipains (B), mature Lys-gingipain (C) and PG27 (D).

83K31, 83K32, 83K36, 83K37 and 83K13 (Fig. 2D, lanes 10, 9, 5, 4 and 12). Deletion mutations in 83K30, 83K33, 83K34 and 83K35 resulted in little production of PG27.

PG0027 gene expression by 83K34

To determine whether or not the small production of PG27 in 83K34 is the result of *PG0027* mRNA instability, *PG0027* mRNA abundance in 83K34 was assessed. As shown in Fig. 3, RT-PCR analysis showed that the PCR bands for *PG0027* were similar between W83 and 83K34, suggesting that *PG0027* mRNA levels were comparable between W83 and 83K34. The following observations lend support to this RT-PCR result. (i) Total RNA from 83K10 showed no *PG0027* band, (ii) All total RNA samples showed similar 16S rRNA band patterns, and (iii) After treatment with RNase A, none of the total RNA samples showed a PCR band. Therefore, we concluded that the C-terminally truncated PG27 protein in 83K34 was unstable and degraded rapidly.

Isolation of suppressor mutants and construction of suppressor/deletion double mutants of PG27

To characterize the defect in PG27 production in PG27 deletion mutants more precisely, we isolated spontaneous suppressor mutants of PG27 deletion mutants. We used GA agar because the growth of *P. gingivalis* in GA medium is strictly dependent on its gingipain activities (Oda *et al.*, 2007). Colony-forming clones on GA agar were isolated during a 2-month incubation period in anaerobic conditions, and we obtained 27 suppressor mutants and four suppressor mutants from 83K34 and 83K35, respectively. No suppressor clones were detected in 83K10, 83K13, 83K27, 83K28, 83K29, 83K30, 83K31, 83K32 or 83K33. Four 83K34 suppressor mutants (83K34R1–83K34R4) and four 83K35 suppressor mutants (83K35R1–83K35R4) were subjected to DNA sequence analysis. 83K34R1–83K34R3 and 83K35R1–83K35R3 harboured one intragenic mutation in the *PG0027* gene, whereas 83K34R4 and 83K35R4 carried no additional mutations in the *PG0027* gene, indicating that 83K34R4 and 83K35R4

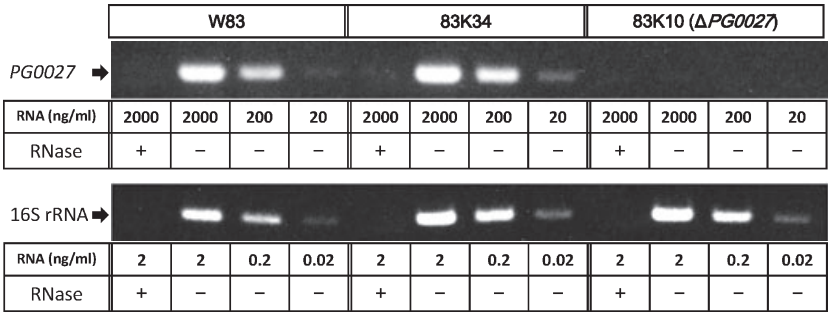

Figure 3 Reverse transcription polymerase chain reaction (PCR) analysis. Gene expression of *PG0027* (upper panel) and the 16S ribosomal RNA gene (lower panel) in W83, 83K34 and 83K10. Total RNAs (RNA; 2000–0.02 ng ml^{-1}) or total RNAs that were treated with RNase A (RNase) were reverse transcribed and amplified. PCR products were separated by 0.75% agarose gel electrophoresis, and visualized by staining with ethidium bromide.

have extragenic suppressor mutations. 83K35R1 carries a frame-shift mutation that deleted the nucleotide sequence GCTT in the 3′-terminal region of the *PG0027* gene of 83K35. The resulting mutation changed the C-terminus Ala380 of PG27 to Arg380-Tyr381-Pro382-Arg383. 83K35R2 and 83K35R3 carry the same frame-shift mutations that inserted the additional nucleotide sequence TAT in the 3′-terminal region of the *PG0027* gene of 83K35. The resulting insertion adds a Tyr381 residue to the C-terminus Ala380 of PG27. This deletion mutation and insertion mutation were introduced into W83, constructing suppressor/deletion double mutants 83K40 and 83K41 (Fig. 4A). 83K34R1 carries a missense mutation that changes the GCT nucleotide sequence for Ala359 of PG27 to the GTT for Val359 (A359V). 83K34R2 and 83K34R3 carry the same missense mutations that change the GCC nucleotide sequence for Ala346 of PG27 to the GTC for Val346 (A346V). Two mutations (either A346V or A359V and an original deletion mutation of 83K34) were introduced into W83 simultaneously, constructing suppressor/deletion double mutants 83K38 and 83K39 (Fig. 4B). As shown in Fig. 4(C), 83K38, 83K39, 83K40 and 83K41 formed black-pigmented colonies on blood agar.

Characterization of suppressor/deletion double mutants of PG27

We determined the gingipain activity in cell extract fractions and extracellular fractions of suppressor/deletion double mutants. As shown in Fig. 5(A), the gingipain activities in both fractions were increased in suppressor/deletion double mutants. Western blot analysis using anti-RgpB antiserum showed that 42-kDa and 70–90-kDa Arg-gingipains were detected in 83K39, 83K40 and 83K41 (Fig. 5B, lanes 6, 3 and 4), comparably to those in 83K12 (lane 1). 83K38 also produced a similar but a somewhat smaller amount of Arg-gingipain bands accompanying 45-kDa abnormal protein bands (Fig. 5B, lane 5). Immunoblot analysis using anti-Kgp showed that 83K12, 83K38, 83K39, 83K40 and 83K41 produced similar 47-kDa Lys-gingipain protein bands (Fig. 5C, lanes 1, 5, 6, 3 and 4), suggesting that the secretion of Lys-gingipains is restored in 83K38, 83K39, 83K40 and 83K41. As the Lys-gingipain activity in the extracellular fraction from 83K38 was low (23% of that of 83K12; Fig. 5A), the 47-kDa Lys-gingipain protein band (Fig. 5C, lane 5) may exhibit reduced activity.

We prepared total membrane fractions from the suppressor/deletion double mutants and subjected them to Western blot analysis using anti-PG27 antiserum (Fig. 5D). 83K12 produced a 39-kDa PG27 protein product in the total membrane fraction (Fig. 5 D, lane 1). Similar protein bands were detected comparably in fractions from 83K39 and 83K40 (lanes 6 and 3). 83K38 and 83K41 produced reduced amounts of similar protein bands in the total membrane fractions (Fig. 5D, lanes 5 and 4). As 83K34 and 83K35 produced no stable PG27 protein (Fig. 2 D, lanes 7 and 6), the suppressor mutations restored production or stability of PG27.

Construction and characterization of PG27-A359V/deletion double mutants

Suppressor/deletion double mutant 83K39 carries A359V and ΔAla380–His391 mutations, and fully recovers the defects of both gingipain generation and

Figure 4 (A, B) Suppressor/deletion double mutants of 83K35 (A) and 83K34 (B). The nucleotide sequence (upper line) and its corresponding amino acid sequence (lower line) are indicated. The deletion mutation (83K40) and insertion mutation (83K41) are depicted in red and in blue (A). Point mutations in 83K38 and 83K39 are depicted in green and in purple (B). *Alw*NI recognition sequences are indicated by underlined nucleotide sequences of 83K35 (A) and 83K34 (B). (C) Accumulation of black pigmentation of suppressor mutants of 83K35 (83K40 and 83K41), suppressor mutants of 83K34 (83K38 and 83K39), A359V single mutant (83K42), A359V/deletion double mutations (83K43–83K47), Δ*PG0027* mutant (83K10), insertion control (83K12) and wild-type (W83), grown on blood agar.

PG27 production. To determine whether the A359V mutation suppresses the other PG27-defective deletion mutations or not, the effect of the A359V mutation on each deletion mutation from 83K30, 83K31, 83K32, 83K33 and 83K35 was investigated. 83K43, 83K44, 83K45, 83K46 and 83K47 are A359V/deletion double mutants, carrying A359V/ΔArg376–His391, A359V/ΔPhe377–His391, A359V/ΔThr378–His391, A359V/ΔLeu379–His391 and A359V/ΔPhe381–His391, respectively. 83K42 carries an A359V mutation, and was used as control for the double mutants. As shown in Fig. 4(C), 83K42 formed black-pigmented colonies, whereas 83K43–47 formed white colonies on blood agar. In 83K42, the activities of Arg-gingipains and Lys-gingipain were comparable in the extracellular fractions (79 and 105% of those 83K12; Fig. 5A) but reduced significantly ($P < 0.01$) by half in cell extract fractions (55 and 54% of those of 83K12), indicating that A359V results in a negative effect on the biogenesis of gingipains in 83K42. In Western blot analysis, 83K42 produced 42-kDa and 70–90-kDa Arg-gingipains (Fig. 5B, lane 7), 47-kDa Lys-gingipain (Fig. 5C, lane 7) and 39-kDa PG27 (Fig. 5D, lane 7). In contrast, 83K43–83K47 showed significantly reduced gingipain activity in both cell extract fractions and extracellular fractions (<3%, $P < 0.01$; Fig. 5A). Importantly, 83K43–83K46 produced 38-kDa and 33-kDa PG27 bands (Fig. 5D, lanes 12–9) but 83K47 produced no PG27 band (lane 8). Therefore, the A359V mutation partly restored the

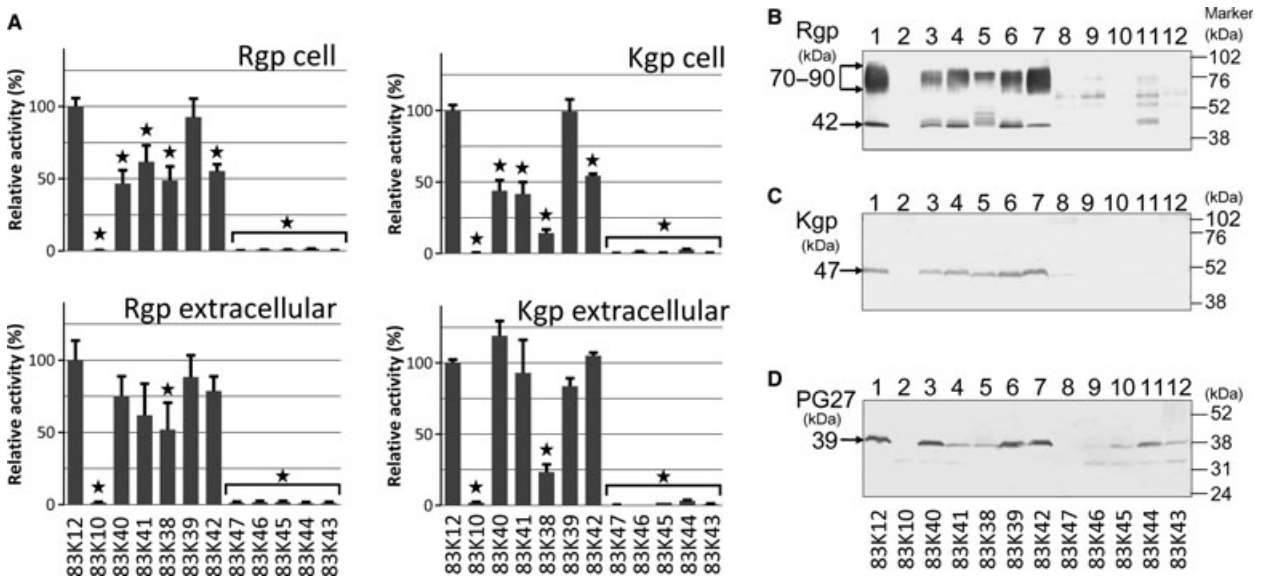

Figure 5 Gingipain expression (A–C) and PG27 expression (D) in suppressor/deletion double mutants. (A) Activities of Arg-gingipains (Rgp) and Lys-gingipain (Kgp) in cell extract fractions (cell) or extracellular fractions (extracellular). Six measurements were collected from two experiments. Error bars indicate SD (calculated from the enzyme activity). *Significant difference compared with 83K12, $P < 0.01$. Protease activity is indicated relative to 83K12 (set at 100%); the absolute values of Rgp/cells, Rgp/extracellular, Kgp/cells and Kgp/extracellular are 83.8, 31.8, 9.86 and 3.13 $\Delta A_{405}\ h^{-1}\ ml^{-1}\ OD_{600}{}^{-1}$, respectively. (B–D) Extracellular fractions (B, C) or total membrane fractions (D) were subjected to 10% sodium dodecyl sulphate–polyacrylamide gel electrophoresis, followed by immunoblot analysis with anti-Rgp antiserum (B), anti-Kgp antiserum (C), or anti-PG27 antiserum (D). Molecular mass markers are on the right. Arrows on the left are the positions of mature Arg-gingipains (B), mature Lys-gingipain (C), and PG27 (D).

stability of PG27 of deletion mutants, but did not suppress the defect in the generation of gingipains.

Orientation of the C-terminal portion of PG27

To determine the orientation of the C-terminal portion of PG27, a histidine-tag was introduced to the C-terminus of PG27, constructing 83K48. The activities of Arg-gingipains and Lys-gingipain in cell extract fractions and extracellular fractions from 83K48 were similar to those from 83K12 (86–103%), indicating that the insertion of the histidine-tag to the C-terminus of PG27 had little or no effect on the biogenesis of gingipains. Using Ni^{2+}-chelated Sepharose, histidine-tagged PG27 was recovered from the cell extract from 83K48 (Fig. 6, lane 5). PG27 contains a surface-exposed region because exposure to proteinase K resulted in no recovery of PG27 (Fig. 6, lane 3). There are six basic amino acid residues that are not embedded in strands of a structure model for PG27. Lys72 is located in loop L1 (between strands S1 and S2). Arg167, Arg170 and Lys197 are located in loop L5. These four residues are on the same side in a PG27 model. In contrast, Lys324 and Arg387 are located in loop L10 and the C-terminal region, respectively, but are on the opposite side to Lys72, Arg167, Arg170 and Lys197 in a PG27 model. Lysine and arginine residues are probably hydrolysed by trypsin if they are in the surface-exposed region of PG27, but are resistant to trypsin if they are within the cell. In case trypsin digestion occurs at Lys324 or Arg387, peptide fragments <10-kDa derived from histidine-tagged PG27 are recovered using Ni^{2+}-chelated Sepharose (but hardly detected in these experimental conditions). If trypsin digestion occurs at Lys72, Arg167, Arg170 and Lys197, 37-, 27-, 26- and 24-kDa peptide fragments are expected. However, exposure of 83K48 cells to trypsin showed no effect on the recovery of PG27 (Fig. 6, lane 1), suggesting that the surface-exposed region of PG27 is resistant to trypsin. Lysine and arginine residues in the surface-exposed region of PG27 evolved to be resistant to gingipains that are trypsin-activity-like proteases. As a result of this, it is thought that these basic amino acid residues also came to show tolerance to trypsin. When 83K48 cells were permea-

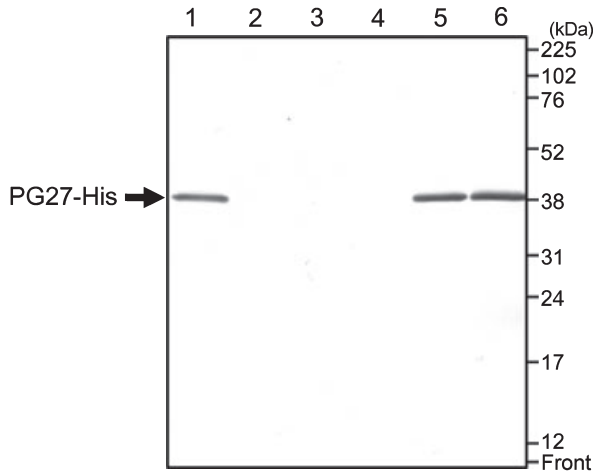

Trypsin	+	+	–	–	–	–
Proteinase K	–	–	+	+	–	–
Triton X-100	–	+	–	+	–	+

Figure 6 Orientation of the C-terminal portion of PG27. Histidine-tagged PG27 or its C-terminal hydrolysates were purified from 83K48 cells that were treated with trypsin or proteinase K in PBS or PBS/Triton X-100 using Ni^{2+}-Sepharose under denaturing conditions, separated by 10% sodium dodecyl sulphate–polyacrylamide gel electrophoresis followed by Western blot analysis using anti-PG27 antiserum.

bilized with Triton X-100, exposure to trypsin resulted in no recovery of the protein band (Fig. 6, lane 2), suggesting that a basic amino acid residue that is sensitive to trypsin but protected within the cell is Lys324 or Arg387. Therefore, a C-terminal portion of PG27 is likely to be located in the periplasmic space (Fig. 7).

DISCUSSION

In our previous study, we found that PG27 was detected both in the outer membrane fraction and in the inner membrane fraction; however, our results implied that PG27 is exposed on the cell surface by cell surface biotinylation experiments (Ishiguro *et al.*, 2009). Now however, there are valid reasons to conclude that PG27/LptO is an outer membrane protein as follows. (i) LptO is detected in highly purified outer membrane vesicles (Chen *et al.*, 2011), (ii) PG27 was degraded by exposure to extracellular proteinase K (Fig. 6, lane 3), and (iii) LptO shows structural similarity with the outer membrane protein FadL (Chen *et al.*, 2011). In the present study, we explored the structure–activity relationships of PG27 by investigating PG27 deletion mutants and suppressor/deletion double mutants. 83K36 (ΔAsp382–His391) showed gingipain activity and secretion of gingipains (Fig. 2 A–C, lane 5), indicating that the C-terminal portion, Asp382–His391, of PG27 is dispensable for the function of PG27. In contrast, 83K32 (ΔThr378–His391) produced PG27 but was defective for the generation of gingipains (Fig. 2A–C, lane 9), suggesting that the region Thr378–His391 of PG27 contains essential residues for the function, but not stability, of PG27. Therefore, the residues Thr378-Leu379-Ala380-Phe381 of PG27 may be essential for the function of PG27. 83K34 (ΔAla380–His391), on the other hand, showed low gingipain activity (Figs 1C and 2A) and produced a small amount of gingipains (Fig. 2B,C, lane 7), but produced no detectable PG27 (Fig. 2D, lane 7), suggesting that Ala380 and Phe381 are probably required for the stability of PG27. We also found that the A359V mutation sufficiently suppresses the gingipain-defective phenotype of 83K34 (83K39: Figs 4B,C and 5A–C, lane 6). We think that A359V affects the stability rather than function of PG27 in 83K34 because the instability of PG27 found in 83K34 (ΔAla380–His391), 83K33 (ΔLeu379–His391) and 83K30 (ΔArg376-His391) was suppressed by A359V (as in 83K39, 83K46 and 83K43: Fig. 5D, lanes 6, 9 and 12), but gingipain-defective phenotypes of the deletion mutants tested – 83K35 (ΔPhe381–His391) and 83K33–83K30 – were not suppressed by A359V (as in 83K47 and 83K46–83K43: Figs 4C and 5A–C, lanes 8, and 9–12). Therefore, Thr378 and Leu379 are essential for the function of PG27 whereas Ala380 and Phe381 are required for its stability.

These results were applied to a predicted β-barrel model for PG27 (Fig. 7). In the dispensable C-terminal portion of PG27 (Asp382–His391), Asp382–Gly385 are in the terminal portion of strand S14 (Fig. 1B), suggesting that about two-thirds of S14 is required to maintain its structure (Asn369–Phe381). The essential residues of PG27, Thr378, Leu379, Ala380 and Phe381, are in the near-centre region of strand S14 (Fig. 1B). Therefore, deletion from the C-terminus His391 to the near centre of strand S14 may result in instability of the β-structure, causing degradation (ΔAla380–His391 or ΔPhe381–His391) or non-functionality of PG27 (ΔThr378–His391 or

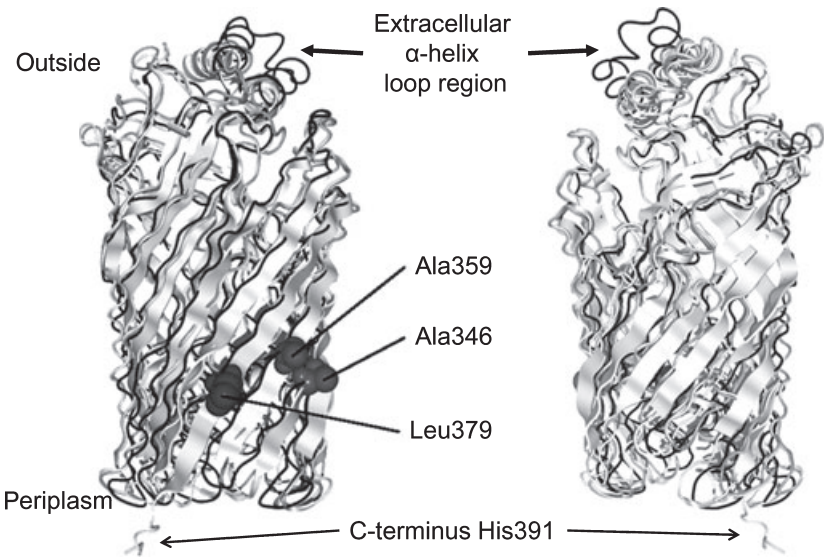

Figure 7 Superposition of model structures of PG27. Side views of PG27 from the front (left) and back (right). Wild-type PG27 is depicted by a ribbon diagram. Three PG27 mutants are depicted by thin tube diagrams [ΔAla380–His391 (black), A346V/ΔAla380–His391 (silver), and A359V/ΔAla380–His391 (white)], and superimposed on the wild-type structure. Ala346, Ala359, Leu379 and His391 are depicted by space-filling models.

ΔLeu379–His391). The defect in 83K35 (ΔPhe381–His391) is suppressed by an intragenic frame-shift mutation that changes the C-terminus Ala380 to Arg380-Tyr381-Pro382-Arg383, or Ala380 to Ala380-Tyr381 (Fig. 4A). The two mutations are different except the 381 tyrosine residue. It should be noted that 83K36 (ΔAsp382–His391) contains a 381 phenylalanine residue at the C-terminus, and has normal generation of gingipains. Because phenylalanine and tyrosine are similar in structure, and are often found in β-strand structures (Walther *et al.*, 2009), Tyr381 may be substituted for Phe381 in strand S14. In contrast, the defect of 83K34 (ΔAla380–His391) is suppressed by the intragenic point mutations A346V (83K38; Fig. 4B) or A359V (83K39; Fig. 4B). In a structural model of PG27, Leu379 (the C-terminus of PG27 in 83K34), Ala359 and Ala346 are located in strands S14, S13 and S12, respectively, but positioned in close proximity to one another (Fig. 7). Molecular modelling was thus used to investigate the predicted structures of 83K34, 83K38 and 83K39. The structure of 83K34 is predicted to be similar to that of the wild-type, except that the positions of two α-helices in the extracellular loop L5 between strands S5 and S6 (Ala163-Tyr198) are shifted about 10° in both vertical and horizontal directions. The observed distortion in L5 is predicted to be mostly restored in 83K38 and 83K39 (Fig. 7), suggesting that the distortion of the extracellular loop L5 contributes to the instability of PG27. Loop L5 contains three basic amino acid residues (Arg167, Arg170 and Lys197). The distorted L5 in 83K34 may cause sensitivity to proteases and be readily degraded.

A proposed role of PG27/LptO is the *O*-deacylation of A-LPS (LPS contains anionic polysaccharide repeating units of phosphorylated branched mannan) by the extracellular domain, and recovery of the released fatty acid chains through the pore. The deacylated A-LPS is then conjugated to secreted C-terminal domain proteins such as gingipains in a coordinated secretion manner via PorSS (Chen *et al.*, 2011). PorSS involves PorK, PorL, PorM, PorN, PorP, PorT, PorW and Sov (Sato *et al.*, 2005, 2010; Saiki & Konishi, 2007); however, their precise roles in the secretion of C-terminal domain proteins have yet to be determined. Other proteins with possible functions in gingipain secretion or processing include PorU, PorQ and PG534 (Saiki & Konishi, 2010b; Sato *et al.*, 2010). Elucidation of the functional roles of these protein factors will shed light on the secretion mechanism of gingipains. Sato *et al.* (2010) suggested that PorK, PorL, PorM, PorN and PorP form a protein complex. In this study, we identified two extragenic suppressor mutants, 83K34R4 and

83K35R4. Further study of these mutations may help in the discovery of proteins that interact with PG27. The isolation and investigation of extragenic suppressor mutants of other protein factors will be important for determining the quaternary structure of this novel secretion machine.

REFERENCES

Abaibou, H., Chen, Z., Olango, G.J. *et al.* (2001) *vimA* gene downstream of *recA* is involved in virulence modulation in *Porphyromonas gingivalis* W83. *Infect Immun* **69**: 325–335.

Banbula, A., Mark, P., Bugno, M. *et al.* (1999) Prolyl tripeptidyl peptidase from *Porphyromonas gingivalis*. *J Biol Chem* **274**: 9246–9252.

Banbula, A., Bugno, M., Goldstein, J. *et al.* (2000) Emerging family of proline-specific peptidases of *Porphyromonas gingivalis*: purification and characterization of serine dipeptidyl peptidase, a structure and functional homologue of mammalian prolyl dipeptidyl peptidase IV. *Infect Immun* **68**: 1176–1182.

Banbula, A., Yen, J., Oleksy, A. *et al.* (2001) *Porphyromonas gingivalis* DPP-7 represents a novel type of dipeptidylpeptidase. *J Biol Chem* **276**: 6299–6305.

van den Berg, B., Black, P.N., Clemons, W.M. Jr and Rapoport, T.A. (2004) Crystal structure of the long-chain fatty acid transporter FadL. *Science* **304**: 1506–1509.

Chen, Y.-Y., Cross, K.J., Paolini, R.A. *et al.* (2002) CPG70 is a novel basic metallocarboxypeptidase with C-terminal polycystic kidney disease domains from *Porphyromonas gingivalis*. *J Biol Chem* **277**: 23433–23440.

Chen, Y.-Y., Peng, B., Yang, Q. *et al.* (2011) The outer membrane protein LptO is essential for the *O*-deacylation of LPS and the co-ordinated secretion and attachment of A-LPS and CTD proteins in *Porphyromonas gingivalis*. *Mol Microbiol* **79**: 1380–1401.

Christersson, L.A., Fransson, C.L., Dunford, R.G. and Zambon, J.J. (1992) Subgingival distribution of periodontal pathogenic microorganism in adult periodontitis. *J Periodontol* **63**: 418–425.

Curtis, M.A., Kuramitsu, H.K., Lantz, M. *et al.* (1999) Molecular genetics and nomenclature of proteases of *Porphyromonas gingivalis*. *J Periodontal Res* **34**: 464–472.

Darveau, R.P. (2010) Periodontitis: a polymicrobial disruption of host homeostasis. *Nat Rev Microbiol* **8**: 481–490.

Hasegawa, Y., Nishiyama, S., Nishikawa, K. *et al.* (2003) A novel type of two-component regulatory system affecting gingipains in *Porphyromonas gingivalis*. *Microbiol Immunol* **47**: 849–858.

Ishiguro, I., Saiki, K. and Konishi, K. (2009) PG27 is a novel membrane protein essential for a *Porphyromonas gingivalis* protease secretion system. *FEMS Microbiol Lett* **292**: 261–267.

John, B. and Sali, A. (2003) Comparative protein structure modelling by iterative alignment, model building and model assessment. *Nucleic Acids Res* **31**: 3982–3992.

Melo, F., Sánchez, R. and Sali, A. (2002) Statistical potentials for fold assessment. *Protein Sci* **11**: 430–448.

Nakayama, K. (1997) Domain-specific rearrangement between the two Arg-gingipain-encoding genes in *Porphyromonas gingivalis*: possible involvement of nonreciprocal recombination. *Microbiol Immunol* **41**: 185–196.

Oda, H., Saiki, K., Numabe, Y. and Konishi, K. (2007) Effect of γ-immunoglobulin on the asaccharolytic growth of *Porphyromonas gingivalis*. *J Periodontal Res* **42**: 438–442.

Oda, H., Saiki, K., Tonosaki, M., Yajima, A. and Konishi, K. (2009) Participation of the secreted dipeptidyl and tripeptidyl aminopeptidases in asaccharolytic growth of *Porphyromonas gingivalis*. *J Periodontal Res* **44**: 362–367.

Potempa, J., Pike, R. and Travis, J. (1995) The multiple forms of trypsin-like activity present in various strains of *Porphyromonas gingivalis* are due to the presence of either Arg-gingipain or Lys-gingipain. *Infect Immun* **63**: 1176–1182.

Saiki, K. and Konishi, K. (2007) Identification of a *Porphyromonas gingivalis* novel protein Sov required for the secretion of gingipains. *Microbiol Immunol* **51**: 483–491.

Saiki, K. and Konishi, K. (2010a) The role of Sov protein in the secretion of gingipain protease virulence factors of *Porphyromonas gingivalis*. *FEMS Microbiol Lett* **302**: 166–174.

Saiki, K. and Konishi, K. (2010b) Identification of a novel *Porphyromonas gingivalis* outer membrane protein, PG534, required for production of active gingipains. *FEMS Microbiol Lett* **310**: 168–174.

Šali, A. and Blundell, T.L. (1993) Comparative protein modelling by satisfaction of spatial restraints. *J Mol Biol* **234**: 779–815.

Sambrook, J., Fritsch, E.F. and Maniatis, T. (1989) *Molecular Cloning: A Laboratory Manual*, 2nd edn. Cold Spring Harbor, NY: Cold Spring Harbor Laboratory.

Sato, K., Sakai, E., Veith, P.D. *et al.* (2005) Identification of a new membrane-associated protein that influences transport/maturation gingipains and adhesion of *Porphyromonas gingivalis*. *J Biol Chem* **280**: 8668–8677.

Sato, K., Kido, N., Murakami, Y. *et al.* (2009) Lipopolysaccharide biosynthesis-related genes are required for colony pigmentation of *Porphyromonas gingivalis*. *Microbiology* **155**: 1282–1293.

Sato, K., Naito, M., Yukitake, H. *et al.* (2010) A protein secretion system linked to bacteroidete gliding motility and pathogenesis. *Proc Natl Acad Sci USA* **107**: 276–281.

Seers, C.H., Slakeski, N., Veith, P.D. *et al.* (2006) The RgpB C-terminal domain has a role in attachment of RgpB to the outer membrane and belongs to a novel C-terminal-domain family found in *Porphyromonas gingivalis*. *Infect Immun* **188**: 6376–6386.

Shen, M. and Sali, A. (2006) Statistical potential for assessment and prediction of protein structures. *Protein Sci* **15**: 2507–2524.

Shi, Y., Ratnayake, D.B., Okamoto, K. *et al.* (1999) Genetic analyses of proteolysis, hemoglobin binding, and hemagglutination of *Porphyromonas gingivalis*. *J Biol Chem* **274**: 17955–17960.

Shoji, M., Ratnayake, D.B., Shi, Y. *et al.* (2002) Construction and characterization of a nonpigmented mutant of *Porphyromonas gingivalis*: cell surface polysaccharide as an anchorage for gingipains. *Microbiology* **148**: 1183–1191.

Socransky, S.S. and Haffajee, A.D. (1992) The bacterial etiology of destructive periodontal disease: current concepts. *J Periodontol* **63**: 322–331.

Takahashi, N. and Sato, T. (2001) Preferential utilization of dipeptides by *Porphyromonas gingivalis*. *J Dent Res* **80**: 1425–1429.

Vanterpool, E., Roy, F. and Fletcher, H.M. (2004) The *vimE* gene downstream of *vimA* is independently expressed and is involved in modulating proteolytic activity in *Porphyromonas gingivalis* W83. *Infect Immun* **72**: 5555–5564.

Vanterpool, E., Roy, F., Sandberg, L. and Fletcher, H.M. (2005a) Altered gingipain maturation in *vimA*- and *vimE*-defective isogenic mutants of *Porphyromonas gingivalis*. *Infect Immun* **73**: 1357–1366.

Vanterpool, E., Roy, F. and Fletcher, H.M. (2005b) Inactivation of *vimF*, a putative glycosyltransferase gene downstream of *vimE*, alters glycosylation and activation of the gingipains in *Porphyromonas gingivalis* W83. *Infect Immun* **73**: 3971–3982.

Walther, D.M., Rapaport, D. and Tommassen, J. (2009) Biogenesis of β-barrel membrane proteins in bacteria and eukaryotes: evolutionary conservation and divergence. *Cell Mol Life Sci* **66**: 2789–2804.